



## CHAPTER IV

### RESULTS AND DISCUSSION

#### 4.1 Effect of Ni Loading

The series of Ni-based catalysts with various Ni loadings were tested for steam reforming of CH<sub>4</sub>, catalyst durability, and carbon deposition.

##### 4.1.1 Activity Test

The Ni/ZSM-5 catalysts with various Ni loadings as 3, 5, 7, 9, 11, and 15 wt% were tested for the catalytic activity on steam reforming of CH<sub>4</sub> under atmospheric pressure and reactants ratio (H<sub>2</sub>O/CH<sub>4</sub>) of 0.8. These activity tests were carried out at 700°C for 5 hours. The catalytic activities of all catalysts are shown in Figures 4.1 to 4.4. In Figure 4.1, CH<sub>4</sub> conversions at 5 hours time-on-stream of supported Ni catalysts are displayed. Conversions are increased with increasing Ni loading up to 11 wt%. At higher Ni loading more than 11 wt%, the catalytic activity of Ni/ZSM-5 catalyst starts to decrease. It is believed that large Ni species on the surface of 15%Ni/ZSM-5 catalyst led to carbon deposition over active metal species, which eventually caused the catalyst deactivation. Moreover, Ni sintering, resulting from large amount of Ni, is another cause of the deactivation. According to these results, which are in a good agreement with work of Roh *et al.* (2003) that studied the influence of Ni loading over NiO/Ce-ZrO<sub>2</sub>/θ-Al<sub>2</sub>O<sub>3</sub> catalysts in the steam reforming of CH<sub>4</sub>. They found that the catalyst with 12 wt% Ni loading exhibited the highest catalytic activity, selectivity and stability. The conversions of CH<sub>4</sub> increased with the rise of Ni loading up to 12 wt% and above this level it decreased. And, they suggested that Ni sintering resulted in relatively low catalytic activity.

From the results, it seems that CH<sub>4</sub> conversion of 3 and 5 wt% Ni (72.21% CH<sub>4</sub> conversion for 3%Ni/ZSM-5 catalyst and 76.19% CH<sub>4</sub> conversion for 5%Ni/ZSM-5 catalyst after 5 hours of reaction) show lower conversion than those of 7 to 15 wt% Ni. But, all of them show slightly decrease in conversions along the time. It is clear that all catalysts remarkably deactivated with time-on-stream, which is most likely due to the carbon formation. As the Ni content increases from 3 to 7 wt%,

the difference of increasing in CH<sub>4</sub> conversion is easy to observe. The catalysts with 7, 9, and 15 wt% do not show significant difference of CH<sub>4</sub> conversions for all testing time. Obviously, during the first period of reaction on 15% Ni/ZSM-5 catalyst, CH<sub>4</sub> conversion shows the increasing step, which may be come from the result of the longer induction period on this catalyst. The aggregation of Ni particles at the high contents of Ni affects the catalyst by taking along time to reach the equilibrium of reaction.

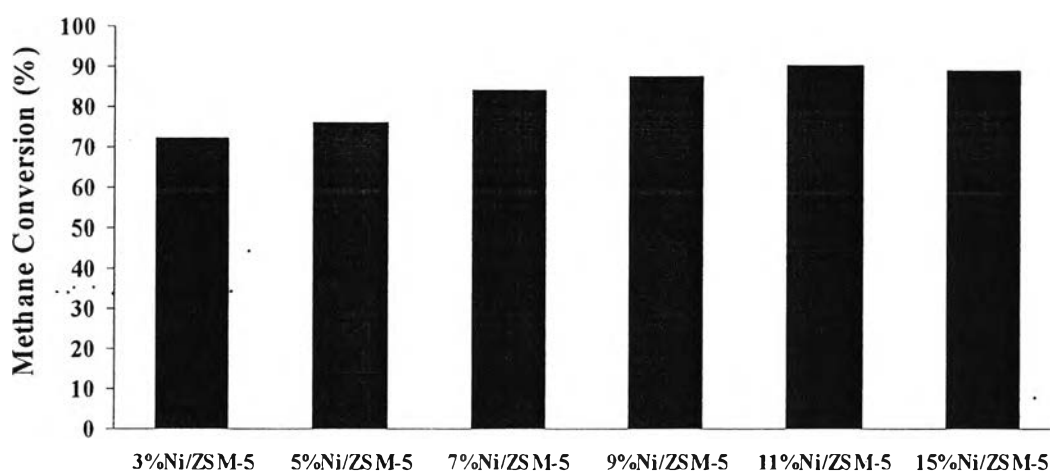


**Figure 4.1** CH<sub>4</sub> conversion at 5 hours time-on-stream over Ni/ZSM-5 catalysts with different Ni loadings for steam reforming reaction at 700°C and H<sub>2</sub>O/CH<sub>4</sub> ratio of 0.8.

H<sub>2</sub> yield at 5 hours time-on-stream is presented in Figure 4.2. It follows the same trend as that of CH<sub>4</sub> conversion. This is due to the fact that the yield of H<sub>2</sub> correlates with CH<sub>4</sub> conversion and H<sub>2</sub> selectivity.

In Figures 4.3 and 4.4, the changes of H<sub>2</sub> selectivity and CO selectivity at the end of reaction time are exhibited, respectively. H<sub>2</sub> selectivity of almost catalysts stays nearly constant at the reaction time of 300 minutes while the selectivity of 3%Ni/ZSM-5 catalyst slightly increases. For the selectivity of CO, it is also constant throughout the testing time over the Ni/ZSM-5 catalysts with the range

of Ni contents about 3 to 15 wt%. CO selectivity of almost catalysts is in a low level which is lower than 10% selectivity.

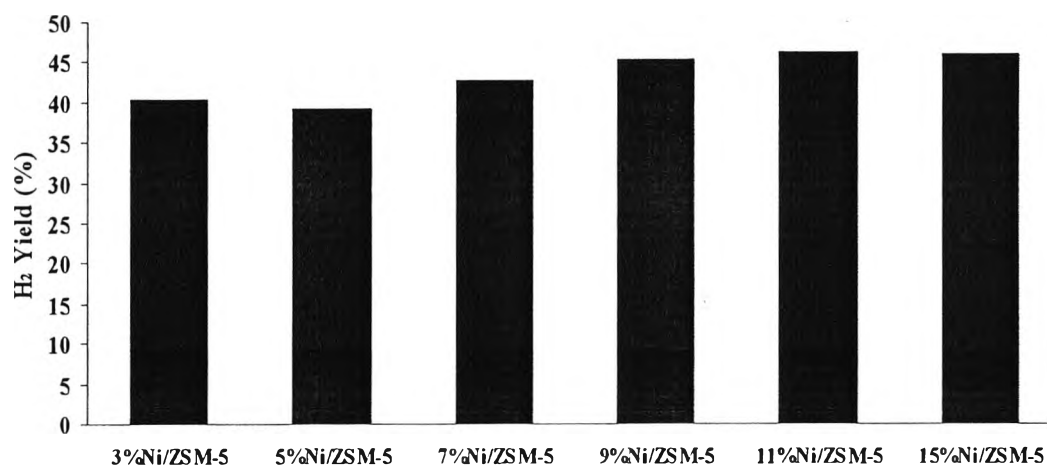


**Figure 4.2** H<sub>2</sub> yield at 5 hours time-on-stream over Ni/ZSM-5 catalysts with different Ni loadings for steam reforming reaction at 700°C and H<sub>2</sub>O/CH<sub>4</sub> ratio of 0.8.

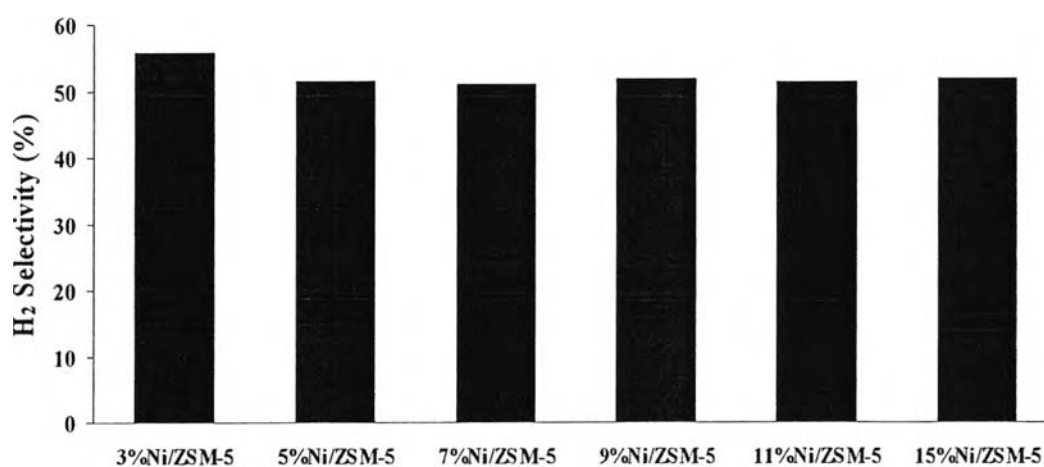


**Figure 4.3** H<sub>2</sub> selectivity at 5 hours time-on-stream over Ni/ZSM-5 catalysts with different Ni loadings for steam reforming reaction at 700°C and H<sub>2</sub>O/CH<sub>4</sub> ratio of 0.8.

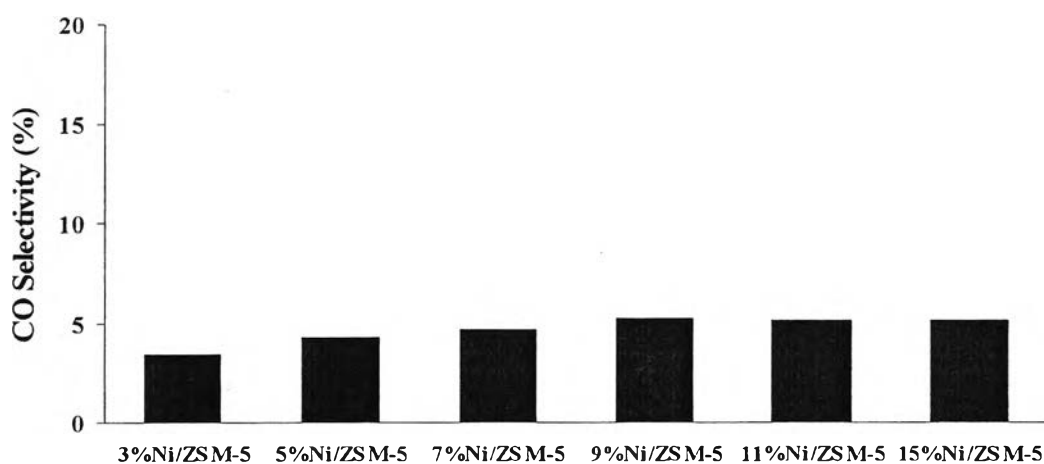


**Figure 4.4** CO selectivity at 5 hours time-on-stream over Ni/ZSM-5 catalysts with different Ni loadings for steam reforming reaction at 700°C and H<sub>2</sub>O/CH<sub>4</sub> ratio of 0.8.

It is not surprising that the activity is a function of the overall Ni content. However, there is an optimum loading beyond which an increase in Ni content does not produce any further significant increase in activity. The optimum Ni loading on the Ni/ZSM-5 catalyst is 11 wt%. It gives 90.47% CH<sub>4</sub> conversion, 46.28% H<sub>2</sub> yield, 51.16% H<sub>2</sub> selectivity, and 5.15% CO selectivity after the reaction occurs for 5 hours. Considering, this amount of Ni loading is used for further studies on CH<sub>4</sub> steam reforming.

#### 4.1.2 Catalyst Characterization

The results from the characterization techniques as X-Ray Diffraction (XRD), Transmission Electron Microscopy (TEM), Thermal Gravimetric Analysis (TGA), Temperature Programmed Oxidation (TPO), and Inductively coupled plasma/optical emission spectrometry (ICP/OES) are revealed in this section. These results belong to the supported Ni/ZSM-5 catalysts with different amount of Ni loadings.

#### 4.1.2.1 Inductively Coupled Plasma/Optical Emission Spectrometry (ICP/OES)

The Perkin-Elmer Optima 4300 DV inductively coupled plasma -optical emission spectrometry was used to determine the actual amounts of metal loading for all catalysts prepared by an impregnation. The ICP results were expressed in Table 4.1. It shows that the Ni supported catalysts with various Ni loadings do not show a significant difference between the actual loading and calculated values. It agrees with the ICP results of Ni/KL reported by Tosiri. However, the actual loadings of almost spent catalysts are lower than that of the fresh catalysts.

**Table 4.1** ICP results of the Ni/ZSM-5 and Ni/Ce/ZSM-5 catalysts

Sample	Metal loading (wt%)			
	Ni	Ce	Al	Si
Fresh 3%Ni/ZSM-5	3.7	-	-	-
Spent 3%Ni/ZSM-5 <sup>a</sup>	2.9	-	-	-
Fresh 5%Ni/ZSM-5	4.9	-	-	-
Spent 5%Ni/ZSM-5 <sup>a</sup>	4.7	-	-	-
Fresh 7%Ni/ZSM-5	7.8	-	-	-
Spent 7%Ni/ZSM-5 <sup>a</sup>	7.2	-	-	-
Fresh 9%Ni/ZSM-5	9.8	-	-	-
Spent 9%Ni/ZSM-5 <sup>a</sup>	9.6	-	-	-
Fresh 11%Ni/ZSM-5	11.9	-	-	-
Spent 11%Ni/ZSM-5 <sup>a</sup>	10.7	-	-	-
Fresh 15%Ni/ZSM-5	15.7	-	-	-
Spent 15%Ni/ZSM-5 <sup>a</sup>	15.1	-	-	-
11%Ni/3%Ce/ZSM-5	11.5	3.5	-	-
11%Ni/5%Ce/ZSM-5	11.2	5.7	-	-
11%Ni/7%Ce/ZSM-5	11.3	7.6	-	-
Spent 11%Ni/ZSM-5 <sup>a</sup>	10.6	-	0.3	77.4
Spent 11%Ni/ZSM-5 <sup>b</sup>	10.3	-	0.3	76.8
Spent 11%Ni/ZSM-5 <sup>c</sup>	10.2	-	0.2	77.9

(a), (b), (c) The catalysts operated on the steam reforming of methane at the H<sub>2</sub>O/CH<sub>4</sub> ratios of 0.8, 1, and 2, respectively.

#### 4.1.2.2 X-Ray Diffraction (XRD)

XRD patterns were recorded by using a Rigaku X-Ray Diffractometer system (RINT-2200) to identify the structure of the catalysts which were performed at different metal loadings.

Figure 4.5 illustrates the XRD patterns of ZSM-5 zeolite and calcined Ni/ZSM-5 catalysts with various Ni loadings of 3, 11, and 15%wt. The XRD patterns of the samples show well crystalline materials corresponding to the MFI structure (Tosheva, 1999). All samples showed the typical pattern peaks identified as NiO peaks, corresponding to the NiO(111) at  $2\theta = 37.3^\circ$ , NiO(200) at  $2\theta = 43.3^\circ$ , and NiO(220) at the  $2\theta$  value of  $63^\circ$  (Matsumura and Nakamori, 2004 and Oh *et al.*, 2003), while the other peaks were attributed to ZSM-5 zeolite. Comparison of XRD profiles of zeolite peaks before and after Ni loading revealed a very small loss of crystallinity in the Ni/ZSM-5 catalysts. The NiO phase in the calcined catalysts suggests the decomposition of nickel nitrate in air at  $700^\circ\text{C}$  for 4 hours to form the NiO species during the preparation of catalysts. According to these XRD patterns of calcined catalysts, the intensity of NiO peaks trends to increase with the increasing Ni content which give more NiO concentration.

The mean crystallite sizes of the NiO crystallite were determined from line broadening calculations using the Scherrer equation for NiO(111), NiO(200), and NiO(220) peaks and the results are reported in Table 4.2. Discernible increases in metal crystallite sizes were observed at the high amounts of Ni loading in comparison with the small amounts of Ni loading.

The XRD patterns of all spent catalysts (Ni loadings of 3, 5, 7, 9, 11, and 15%) are presented in Figure 4.6. Two major XRD peaks, attributed to Ni(111) at  $44.5^\circ$  and Ni(200) at  $51.8^\circ$  (Roh *et al.*, 2003 and Matsumura and Nakamori, 2004), were recorded. After the reaction, the peaks attributed to NiO were diminished and the Ni peaks were intensified, showing that the Ni particles were completely reduced during the reaction, which can be confirmed by the XRD patterns of all reduced catalysts in the appendix B. In the profiles of spent samples, Ni peaks intensity moves forward with the increasing of Ni content.

The Ni crystallite sizes for both reduced and spent catalysts are shown in Table 4.3. They were also determined from the line broadening of the

XRD peaks of Ni(111) and Ni(200). It is seen that the spent catalysts with high amounts of Ni loading show larger metal crystallite sizes than the catalysts with small amounts of Ni loading. And, the metal crystallite sizes of almost spent catalysts are also slightly larger than those of reduced catalysts. These may indicate that Ni particles aggregated during the reaction and Ni sintering occurred. It agrees well with the results of Ni/KL and Ni/NaY reported by Tosiri and Chankam.

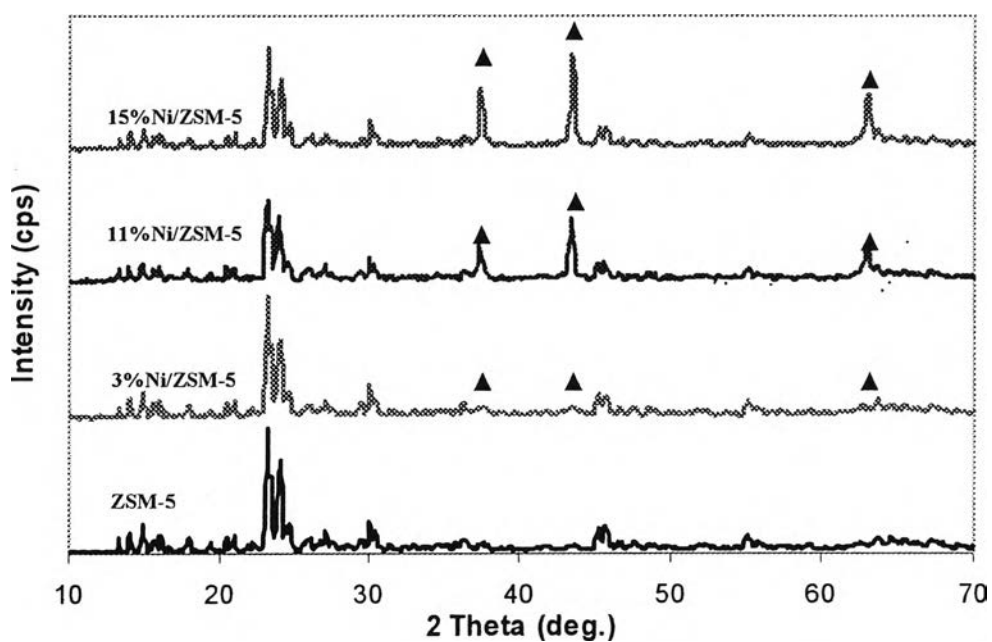


**Figure 4.5** XRD patterns of ZSM-5 zeolite and various amounts of Ni supported on ZSM-5 zeolite catalysts calcined at 700°C for 4 hours; (▲), NiO phase.

**Table 4.2** Metal crystallite sizes of calcined Ni/ZSM-5 catalysts with various amounts of Ni loading

Catalyst	NiO(111) ( $2\theta = 37.3^\circ$ ) (nm)	NiO(200) ( $2\theta = 43.3^\circ$ ) (nm)	NiO(220) ( $2\theta = 63^\circ$ ) (nm)
3%Ni/ZSM-5	12.65	10.04	21.22
11%Ni/ZSM-5	22.91	27.39	21.37
15%Ni/ZSM-5	27.95	26.71	23.47

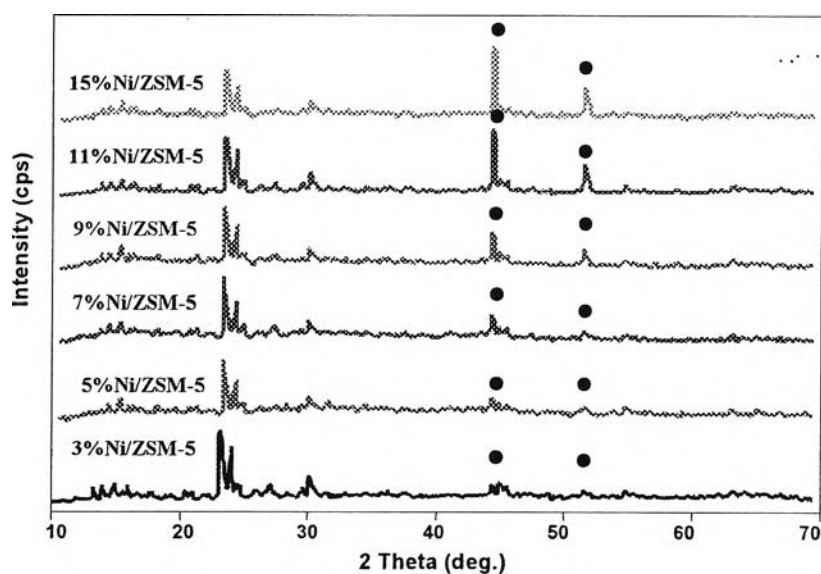


**Figure 4.6** XRD patterns of spent Ni/ZSM-5 catalysts with various loadings of Ni, which operated on steam reforming reaction at 700°C and atmospheric pressure for 5 hours; (●), Ni metal phase.



**Table 4.3** Metal crystallite sizes of both reduced and spent Ni/ZSM-5 catalysts with various amounts of Ni loading

Catalyst	Ni(111) ( $2\theta = 44.5^\circ$ ) (nm)		Ni(200) ( $2\theta = 51.8^\circ$ ) (nm)	
	reduced	spent	reduced	spent
3%Ni/ZSM-5	25.02	27.08	19.84	28.30
5%Ni/ZSM-5	18.99	30.22	13.32	21.59
7%Ni/ZSM-5	32.27	34.33	20.39	22.82
9%Ni/ZSM-5	31.32	33.27	26.13	24.74
11%Ni/ZSM-5	31.21	38.49	21.08	33.96
15%Ni/ZSM-5	35.61	33.79	25.82	30.66

#### 4.1.2.3 Temperature Programmed Oxidation (TPO)

The amount, location, and morphology of carbon deposited on the spent Ni catalysts in activity tests were measured by temperature programmed oxidation (TPO) experiments. It provides direct information regarding coke oxidation rate. Figure 4.7 shows the CO<sub>2</sub> signal as a function of temperature during the TPO experiments performed after 5 hours of reaction time for Ni/ZSM-5 at 700°C. At least three types of carbonaceous species were found to exist on the catalysts, as shown on TPO curves of the spent 3%Ni/ZSM-5, 5%Ni/ZSM-5, 7%Ni/ZSM-5, and 11%Ni/ZSM-5 catalysts after the reactions under normal conditions; the first low temperature peak with high intensity at the range of 350-390°C (except for 3%Ni/ZSM-5 catalyst which has the low intensity at this point), the second peak is observed around 450-550°C and the last one with low intensity at above 600°C. The peaks observed at the range of 350-390°C may be related with surface carbon C<sub>s</sub> as the superficial carbide, which may be the reaction intermediate. The C<sub>s</sub> may be, or develop into, more than one form of carbon (Satterfield, 1991 and Tosiri, 2006). A filamentous or whiskerlike carbon is the second form of carbon

which attributed to the peaks occurring around 450-550°C. And other peaks above 600°C are identified as pyrolytic carbon (Satterfield, 1991). Nevertheless, it is interesting to note that even in the case of the pure amorphous carbon, the TPO peak is non-symmetric. This is an indication that the carbon reaction order is less than one and the peak is more symmetric when the carbon reaction order is one (Querini, 2004), especially in a profile of 7%Ni/ZSM-5 catalyst. For 15%Ni/ZSM-5 catalyst, a first peak is observed at 390°C and a second peak with high intensity is observed at 650°C. On the other hand, the high temperature peak was not observed in the spent 9%Ni/ZSM-5 catalyst and the intensity of a low temperature peak was very small even longer reaction time.

Wang (1998) proposed that there is a relationship between oxidation temperature and the distance between the coke on the support and the metal. Coke on the support is burned at a higher temperature than the coke on the metal. From this Figure, it is clear that the gasification of carbon is more difficult for Ni/ZSM-5 catalysts with high amounts of Ni loading (except 9% Ni loading) due to the longer distance between surface carbon and Ni particles which deposited at inner pores during the impregnation method.

These TPO profiles are related to the amounts of carbon deposited on Ni/ZSM-5 catalysts with various Ni loadings that reported in Table 4.4. It exhibits that the lowest formation of deposited carbon can occur at 9%Ni/ZSM-5 catalyst and the amounts of deposited carbon on the surface are slightly extend with the enhancement of Ni loadings.

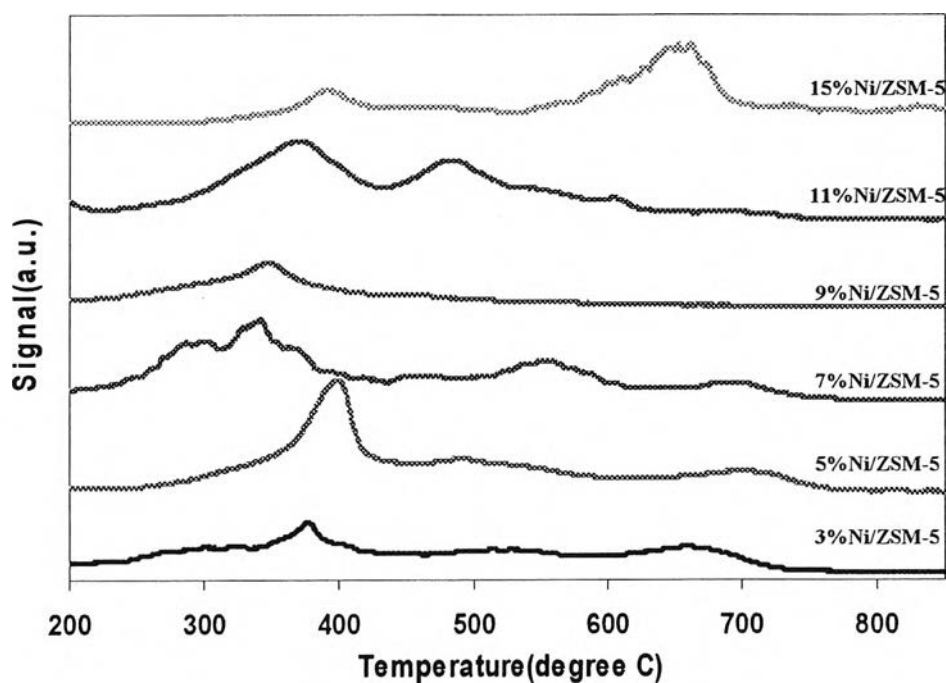


**Figure 4.7** TPO profiles of the Ni/ZSM-5 catalysts with various amounts of Ni loading after 5 hours of reaction at 700°C and atmospheric pressure.

**Table 4.4** Amounts of carbon deposited on Ni/ZSM-5 catalysts with various Ni loadings after 5 hours of reaction, which were characterized by using TPO and TGA techniques

Catalyst	% wt Carbon <sup>(1)</sup>	% wt Carbon <sup>(2)</sup>
3%Ni/ZSM-5	0.40	0.43
5%Ni/ZSM-5	0.56	0.57
7%Ni/ZSM-5	0.51	0.55
9%Ni/ZSM-5	0.21	0.3
11%Ni/ZSM5	0.57	0.53
15%Ni/ZSM-5	0.63	0.68

<sup>(1)</sup> As measured by TPO

<sup>(2)</sup> As measured by TGA

#### 4.1.2.4 Thermal Gravimetric Analysis (TGA)

The catalyst deactivation in this reaction is basically related to the deposition of inactive carbon species on the active metal sites. The amounts of carbon formed on the Ni supported catalysts with various Ni loadings after 5 hours reaction were determined by TGA measurements, which were carried out in an oxygen-containing atmosphere (Table 4.4 on above). TGA results show that the weight losses of all samples tell the amounts of carbon deposited on the surface of Ni/ZSM-5 catalysts. And, almost present TGA results have the intimately %wt carbon values and move on with the identical trends as compared to the results which measured by the TPO technique. Additionally, these TGA results can help to confirm the TPO results for the identification of the catalyst deactivation by coking as a main cause.

#### 4.1.2.5 Transmission Electron Microscopy (TEM)

The localization, nature, and structure of deposited coke have been examined with electron microscopy. In the case where carbon whiskers are formed, there are a large number of studies using this technique. For this technique, the morphology of the carbon deposits is easily distinguished from the catalyst, and the interpretation of the analysis is easier than in other cases where coke is distributed on the surface of the catalyst. And, one of the limitations is that the TEM cannot see non-aromatic functional groups, and therefore each stack can be surrounded by an unknown amount of carbon and considerably enlarge the size of the real carbonaceous individual units (Querini, 2004).

TEM images of the 3%Ni/ZSM-5, 11%Ni/ZSM-5, and 15%Ni/ZSM-5 catalysts reduced at 700°C for 1 hour are shown in Figure 4.8. Many small Ni particles (about 8-53 nm) are observed on the plane of the support for the reduced 3%Ni/ZSM-5 catalyst as shown in Figure 4.8(a). And, Figure 4.8(b) shows that the larger Ni particles with diameters mainly ranging between 21 and 79 nm appeared on the reduced 11%Ni/ZSM-5 catalyst. Obviously, the increase of Ni content resulted in the aggregation of Ni particles. The reduced 15%Ni/ZSM-5 catalyst has a considerably broader particle size distribution relative to the others which appears from 23 to 136 nm (Figure 4.8(c)).

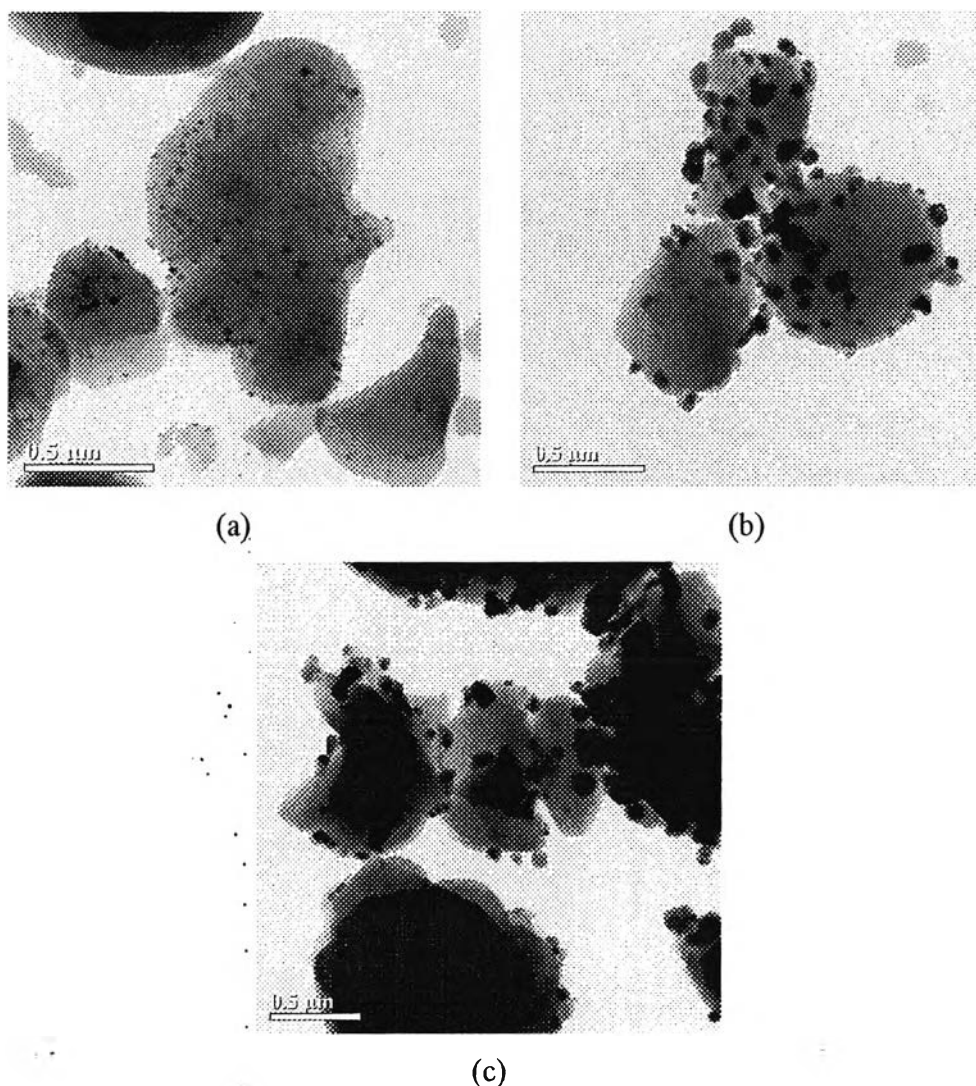


**Figure 4.8** TEM images of the catalysts after H<sub>2</sub> reduction at 700°C; (a) 3%Ni/ZSM-5, (b) 11%Ni/ZSM-5, (c) 15%Ni/ZSM-5.

In order to compare the TEM technique with the XRD technique, the average particle size is calculated according to the equation  $d_s = \frac{\sum n_i d_i^3}{\sum n_i d_i^2}$  on the basis of counting the diameter of numerous particles. The average particle sizes of the reduced 3%Ni/ZSM-5, 11%Ni/ZSM-5, and 15%Ni/ZSM-5 catalysts are 24.18, 60.92, and 95.60 nm, respectively. Judging from the XRD results, the Ni particle sizes which calculated from the Scherrer equation are smaller than those observed by TEM, especially on the high Ni contents catalysts. The differences are probably due to errors or limitations for detecting the small particles of TEM (Canizares *et al.*, 1998). Likewise, the well dispersion of the reduced 3%Ni/ZSM-5

catalyst compared to the reduced 11%Ni/ZSM-5 and 15%Ni/ZSM-5 catalysts can be also observed by Figure 4.8.

Figure 4.9 shows the TEM images of the 3%Ni/ZSM-5, 11%Ni/ZSM-5, and 15%Ni/ZSM-5 catalysts after the reforming reaction at 700°C for 5 hours. The images of all spent catalysts with various Ni loadings did not change much for before and after reaction, indicating that little carbon was formed on these catalyst surfaces during the reaction. But, it perceives that the Ni particles after reaction are greater than before reaction. And, the agglomeration of Ni particles, which grows up with the increasing of Ni contents, is easier to observe. Therefore, considering these results, Ni sintering may be another cause of the deactivation in this catalyst. However, these are concerned with Quincoces *et al.* (2002)'s work that studied the effect of the Mo addition on the Ni/Al<sub>2</sub>O<sub>3</sub> catalysts in dry reforming reaction. Ni sintering at a short time of reaction was found to be a cause of deactivation which can be demonstrated by the TEM images, where an increase in the particles size was observed.

From Figures 4.9(a) and 4.9(b), the size distribution of Ni particles for the spent 3%Ni/ZSM-5 catalyst is around 8-73 nm and the Ni particles of 13-107 nm were mainly observed by TEM on the spent 11%Ni/ZSM-5 catalyst surface. With a broader particle size distribution, the spent 15%Ni/ZSM-5 catalyst expressed the Ni particle diameters as 20-126 nm (Figure 4.9(c)).

Further information comes from the calculation of the average metal particle size with above equation. The average particle sizes of the spent 3%Ni/ZSM-5, 11%Ni/ZSM-5, and 15%Ni/ZSM-5 catalysts are 49.71, 64.67, and 109.68 nm, respectively. These present results by TEM images show a considerable agreement with the results of XRD measurements, which indicated that the metal crystallite sizes of the Ni/ZSM-5 catalysts after reaction are larger than the sizes of catalysts before reaction. Besides, the low dispersion of the Ni/ZSM-5 catalysts after reaction, corresponding to a larger particle, can be observed by these TEM images.

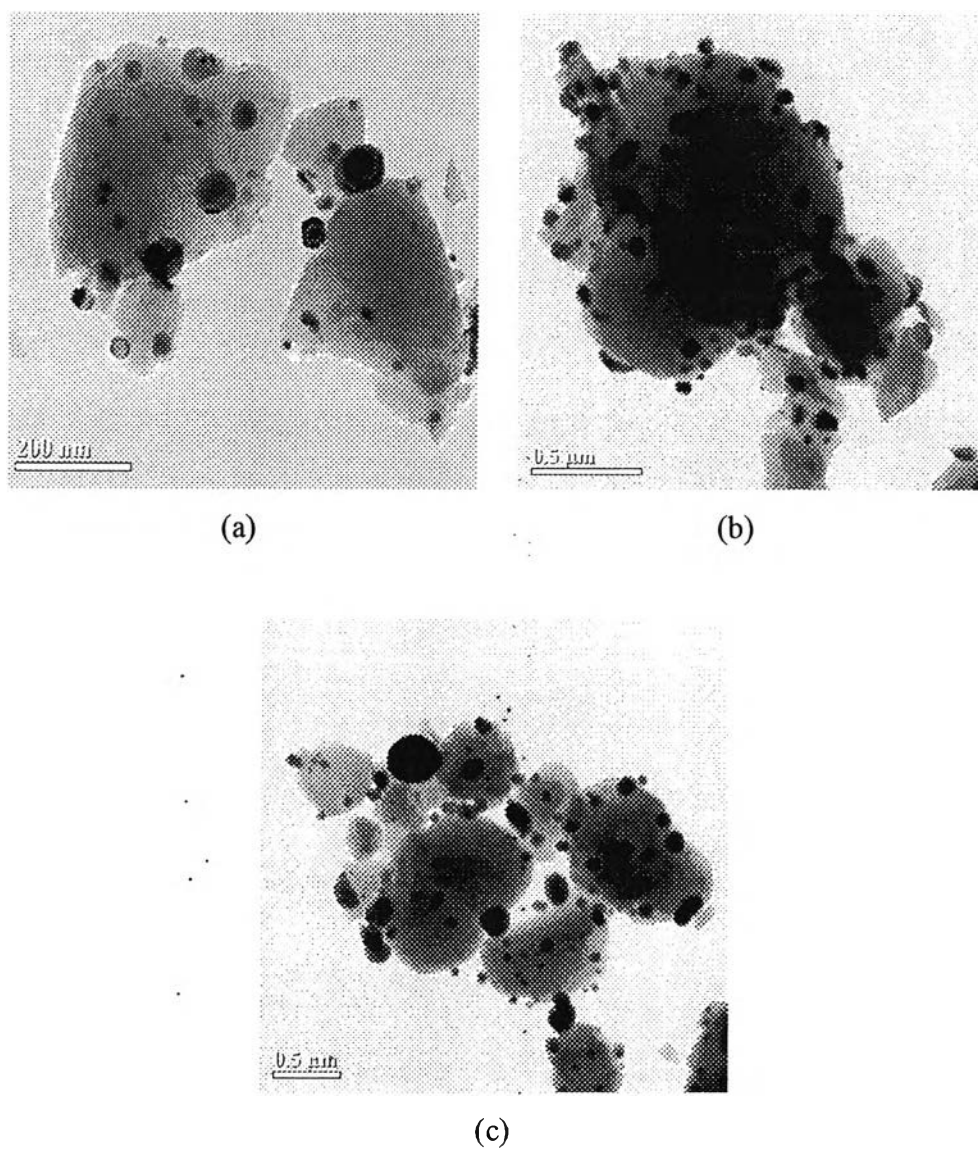


**Figure 4.9** TEM images of the the catalysts after reforming reaction at 700°C; (a) 3%Ni/ZSM-5, (b) 11%Ni/ZSM-5, (c) 15%Ni/ZSM-5.

## 4.2 Effect of Steam-to-Methane Ratio

The series of 11%Ni-based catalysts with various steam-to methane ratios were tested in steam reforming of CH<sub>4</sub>.

### 4.2.1 Activity Test

Since the 11%Ni/ZSM-5 is preferred by steam reforming of CH<sub>4</sub>, the effect of steam-to-methane (H<sub>2</sub>O/CH<sub>4</sub>) ratio on CH<sub>4</sub> conversion, H<sub>2</sub> yield, H<sub>2</sub> selectivity, and CO selectivity is studied over this catalyst. The reactions were fixed at 700°C and atmospheric pressure to obtain a high activity. It was reported that amount of H<sub>2</sub> in the final product is adjustable by increasing the H<sub>2</sub>O/CH<sub>4</sub> ratios; therefore, in this work, three H<sub>2</sub>O/CH<sub>4</sub> ratios of 0.8, 1, and 2 were studied.

CH<sub>4</sub> conversion as a function of time-on-stream is expressed in Figure 4.10. With increasing H<sub>2</sub>O/CH<sub>4</sub> ratio in the feed, the conversions of CH<sub>4</sub> are decreased. Like that a higher H<sub>2</sub>O/CH<sub>4</sub> ratio results in a lower CH<sub>4</sub> conversion. The disagreement between these results and the results from Yamazaki *et al.* (1996)'s study appears. Their study concerned about methane-steam reaction under low steam-to-carbon ratio to develop the stability of Ni catalysts. Yamazaki *et al.* showed that, while the Ni/Al<sub>2</sub>O<sub>3</sub>-MgO revealed good activity and stability with high CH<sub>4</sub> conversion around 98% for more than 40 hours under a steam to carbon ratio of 2, it lost its activity and structure (81% CH<sub>4</sub> conversion at the beginning) and the reactor was plugged due to the coke formation under a steam to carbon ratio of 1 at 750°C and atmospheric pressure.



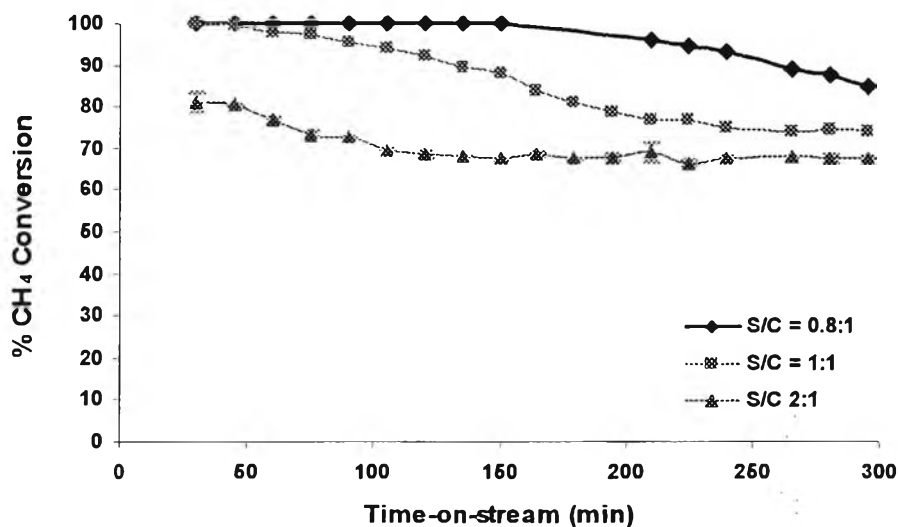


**Figure 4.10** CH<sub>4</sub> conversion as a function of time-on-stream over Ni/ZSM-5 catalysts with different H<sub>2</sub>O/CH<sub>4</sub> ratios for steam reforming reaction at 700°C.

It is apparent that the CH<sub>4</sub> conversions, with respect to either H<sub>2</sub>O/CH<sub>4</sub> ratio of 0.8 or H<sub>2</sub>O/CH<sub>4</sub> ratio of 1 are quite similar for the small declination along a period of catalytic reaction. It shows 84.75% CH<sub>4</sub> conversion for a ratio of 0.8 and 74.05% CH<sub>4</sub> conversion for a ratio of 1, at the end of testing (5 hours). On the contrary, the significant decreasing of CH<sub>4</sub> conversion with the time-on-stream not occurred when the H<sub>2</sub>O/CH<sub>4</sub> ratio was 2. It is noticeable that this result may come from the excess steam in the feed.

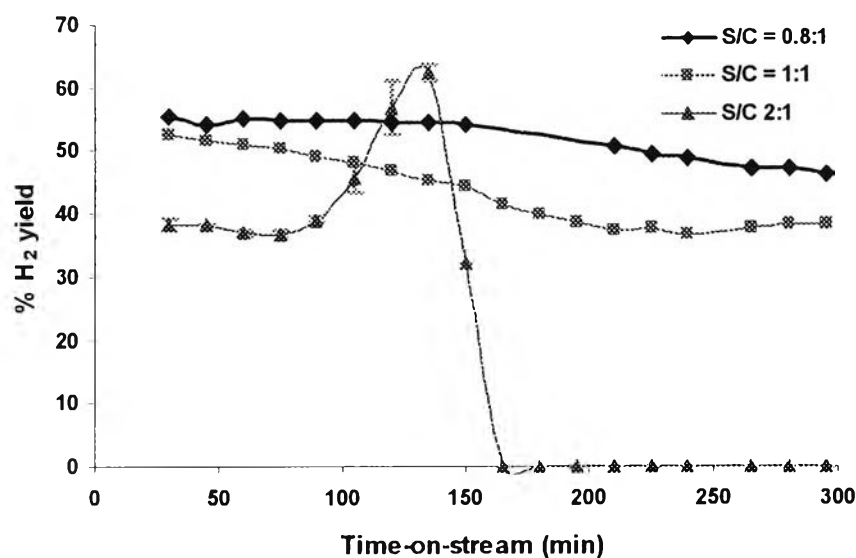
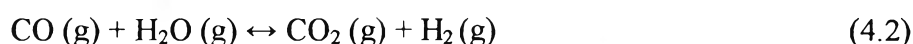
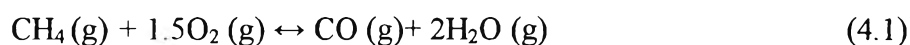


**Figure 4.11** H<sub>2</sub> yield as a function of time-on-stream over Ni/ZSM-5 catalysts with different H<sub>2</sub>O/CH<sub>4</sub> ratios for steam reforming reaction at 700°C.

Figure 4.11 shows the changes of H<sub>2</sub> yield with the time of reaction. During 5 hours of reaction, the reduction of H<sub>2</sub> yield emerges in all different H<sub>2</sub>O/CH<sub>4</sub> ratios studied catalyst. A rising of H<sub>2</sub>O/CH<sub>4</sub> ratio produces a lower level of the yield. At a H<sub>2</sub>O/CH<sub>4</sub> ratio of 1, the initial and the last H<sub>2</sub> yields of 11%Ni/ZSM-5 catalyst are 52.72% and 38.58%, respectively. Besides, the catalyst shows ~55.48% H<sub>2</sub> yield at the beginning and 46.28% H<sub>2</sub> yield at the end under the reactants ratio of 0.8. And 38.40% of H<sub>2</sub> yield suddenly fall to 0% within 165 minutes of reaction at ratio of 2. This obvious stopping of H<sub>2</sub> production on the excess steam condition may be the result of the dealumination in zeolite's structure. Steam greatly enhances the rate of Si-O-Al bond cleavage and removes tetrahedrally coordinated aluminum from the lattice, which increases the accessibility of acid sites (Beyer, 2002). Generally, it is well accepted that acidity of zeolites governs their activity, and the acidity induces the formation of carbon for this case, explaining why the role of dealumination is considered. During the reaction time of 90-150 minutes, H<sub>2</sub> yield of the 11%Ni/ZSM-5 catalyst at a H<sub>2</sub>O/CH<sub>4</sub> ratio of 2 shows a rapid increase compared to the others. This may rely on the formation of H<sub>2</sub> via the water gas shift reaction of CO and water which are produced by the incomplete combustion of CH<sub>4</sub> and the

dissolved oxygen in the water. However, this is not due to leaking corresponding to Laosiripojana *et al.*'s work, it reported that the addition of the oxygen into the steam reforming reaction can increase the conversion of methane, resulting in the disagreement with the results as shown in Figure 4.10. These may help to confirm that the oxygen used in the combustion did not come from the air which concerned to the leaking of the activity test line. Moreover, this CH<sub>4</sub> combustion is another reaction which can occur together with the steam reforming of CH<sub>4</sub> when the system has more dissolved oxygen from water. And, these reactions are expressed in the following equations:



At the same time, the transformation of Ni metal phase may paralleled occur on the catalyst. Ni metal on the catalyst could be reacted with the dissolved oxygen in the water to form NiO according to the following equation:



NiO is an inactive form of this catalyst for the steam reforming reaction. Therefore, the formation of this inactive NiO phase suggests the decrease and dropping of H<sub>2</sub> production after 150 minutes of reaction as shown in H<sub>2</sub> yield graph (Fig. 4.11).

Noticeably, the continue standing of CH<sub>4</sub> conversion for the 11%Ni/ZSM-5 catalyst operated under a H<sub>2</sub>O/CH<sub>4</sub> ratio of 2 after 165 reaction minutes may relate to the formation of CO<sub>2</sub> gas (Fig. 4.14) which could be generated from the combustion of the dissolved oxygen in the water and either the surface carbon of methane or CO from the steam reforming. In consistent with this view, NiO is obtained as in XRD. The formation of CO<sub>2</sub> gas in this way can be explained by the following equation:



And, this reaction can occur over the NiO phase that may explain the continue formation of CO<sub>2</sub> after the appearance of the catalyst deactivation.

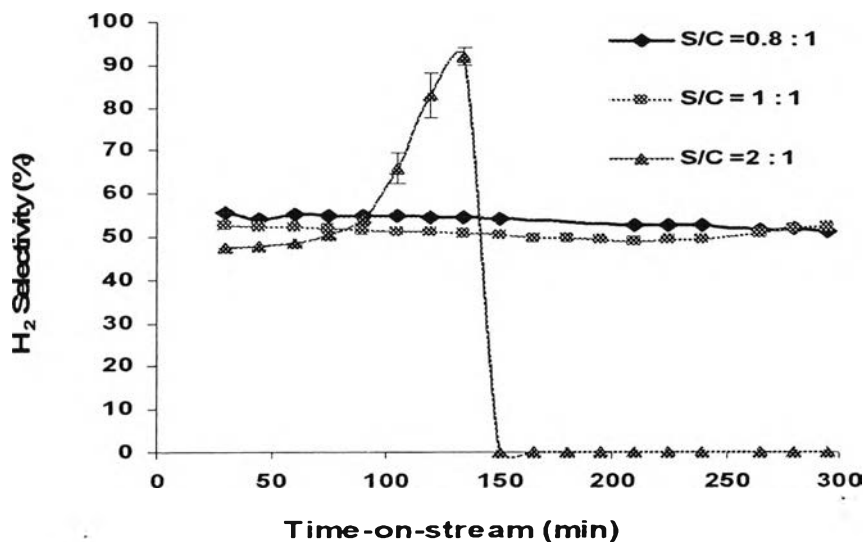


**Figure 4.12** H<sub>2</sub> selectivity as a function of time-on-stream over Ni/ZSM-5 catalysts with different H<sub>2</sub>O/CH<sub>4</sub> ratios for steam reforming reaction at 700°C.

As shown in Figure 4.12, H<sub>2</sub> selectivity of the catalysts remains mostly constant throughout the reaction time at H<sub>2</sub>O/CH<sub>4</sub> ratios of 0.8 and 1. The average value of H<sub>2</sub> selectivity on these ratios is around 50%. Conversely, the 11%Ni/ZSM-5 catalyst at a H<sub>2</sub>O/CH<sub>4</sub> ratio of 2 encounters the deactivation problem which immediately drops H<sub>2</sub> selectivity. It shows the same trend as the H<sub>2</sub> yield of the catalyst at a H<sub>2</sub>O/CH<sub>4</sub> ratio of 2. The increasing of this selectivity at the period of 90-150 minutes may be explained by the formation of H<sub>2</sub> which corresponding to Equations 4.1 and 4.2, respectively. And, the suddenly decrease after 150 minutes of reaction may be explained by the NiO formation as expressed in Equation 4.3. This selectivity reaches the highest point (about 94.93% H<sub>2</sub> selectivity) at the time of 150 min and rapidly falls to 0% H<sub>2</sub> selectivity in the next.

In Figure 4.13, the selectivity of CO is expressed. Although, the operation occurs at different H<sub>2</sub>O/CH<sub>4</sub> ratios, the CO selectivity trends to decrease along 5 hours of the test. Especially, at a H<sub>2</sub>O/CH<sub>4</sub> ratio of 2 which makes the

selectivity stays at much lower point because of the appearance of water gas shift reaction on this condition.

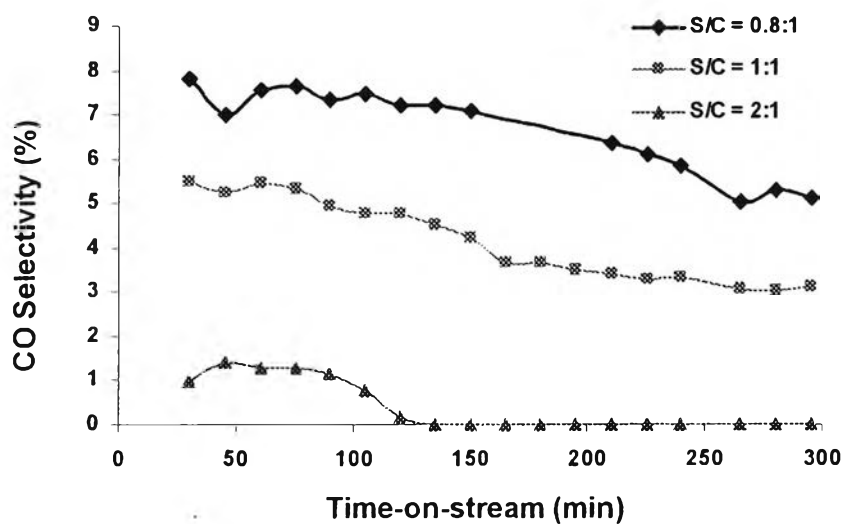


**Figure 4.13** CO selectivity as a function of time-on-stream over Ni/ZSM-5 catalysts with different H<sub>2</sub>O/CH<sub>4</sub> ratios for steam reforming reaction at 700°C.

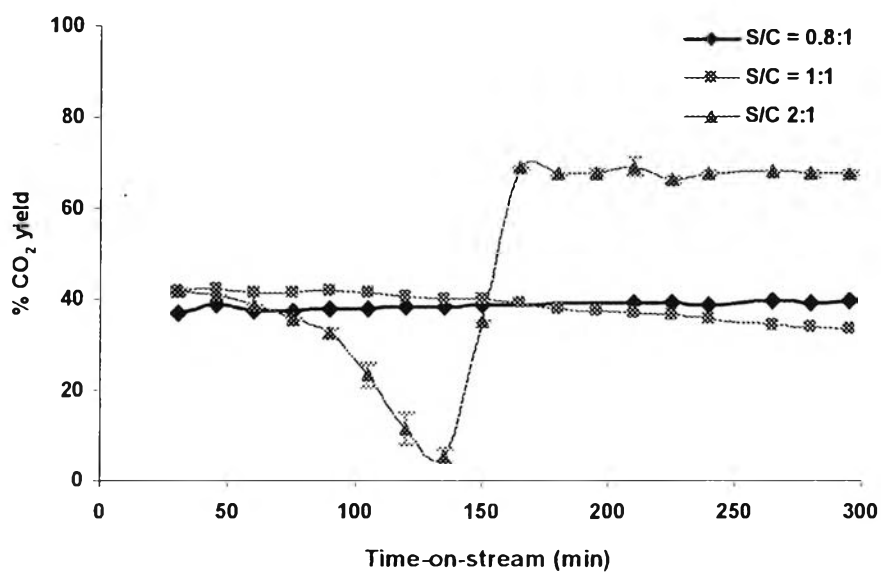


**Figure 4.14** CO<sub>2</sub> yield as a function of time-on-stream over Ni/ZSM-5 catalysts with different H<sub>2</sub>O/CH<sub>4</sub> ratios for steam reforming reaction at 700°C.

The CO<sub>2</sub> yields are expressed in Figure 4.14. CO<sub>2</sub> yield of the catalysts shows the near value throughout the reaction time at H<sub>2</sub>O/CH<sub>4</sub> ratios of 0.8 and 1. However, at a H<sub>2</sub>O/CH<sub>4</sub> ratio of 2, the yield of CO<sub>2</sub> trends to decrease in the time of 90-140 minutes of the test. It may be the result of the reverse conversion into CO by Ni metal on the catalyst surface. After this period, this yield trends to increase and stays continuously constant at the high level until the end. This CO<sub>2</sub> gas is generated from the combustion of the dissolved oxygen in the water and either the surface carbon of methane or CO from the steam reforming as occurred in Equation 4.4.

Hence, based on the above results, it can be concluded that the suitable H<sub>2</sub>O/CH<sub>4</sub> ratio for the reaction of steam reforming over 11%Ni/ZSM-5 catalyst is 0.8. This is due to a higher activity obtained from the activity test.

#### 4.2.2 Catalyst Characterization

The 11%Ni/ZSM-5 catalysts operated at different H<sub>2</sub>O/CH<sub>4</sub> ratios of 0.8, 1, and 2 were characterized by ICP, XRD, TGA, and TPO, respectively. And, the results are expressed in following;

##### 4.2.2.1 *Inductively Coupled Plasma/Optical Emission Spectrometry (ICP/OES)*

Considering at different H<sub>2</sub>O/CH<sub>4</sub> ratios, there are little differences in the %Al and %Si contents of the spent 11%Ni/ZSM-5 catalyst operated at a H<sub>2</sub>O/CH<sub>4</sub> ratio of 2 (Table 4.1), which may be suggested that the dropping of hydrogen production is caused by the dealumination (Beyer, 2002).

##### 4.2.2.2 *X-Ray Diffraction (XRD)*

Figure 4.15 shows the XRD patterns of spent samples (11%Ni loading). The spent samples were applied to methane steam reforming under different stoichiometric feed compositions (H<sub>2</sub>O/CH<sub>4</sub> = 0.8, 1, and 2) for 5 hours. The XRD patterns of spent catalysts show the metallic Ni peaks which assigned to Ni(111) at 44.5° and Ni(200) at 51.8° (Roh *et al.*, 2003 and Matsumura and Nakamori, 2004) and other peaks attributed to ZSM-5 zeolite. The higher H<sub>2</sub>O/CH<sub>4</sub>

ratio gives the lower peak intensity of Ni metal. After steam reaction of 11%Ni/ZSM-5 with the H<sub>2</sub>O/CH<sub>4</sub> ratios of 0.8 and 1 for 5 hours, metallic Ni peaks were detected. This is an evidence that the absolute reduction of Ni particles occurred during the reaction. On the other hand, the XRD pattern of catalyst operated at a H<sub>2</sub>O/CH<sub>4</sub> ratio of 2 exhibits the appearance of NiO peaks with metallic Ni peaks, confirming the formation of inactive form of Ni that reduced the activity in steam reforming.

Table 4.5 reports the metal crystallite sizes of spent 11%Ni/ZSM-5 catalysts which operated on reforming reaction at H<sub>2</sub>O/CH<sub>4</sub> ratios of 0.8, 1, and 2 for 5 hours. The Scherrer equation was used to calculate the crystallite sizes. As observed in Table 4.5, the XRD peaks of Ni(200), the Ni crystallite size of a catalyst operated at the lowest H<sub>2</sub>O/CH<sub>4</sub> ratio is larger than that of the other catalysts (at H<sub>2</sub>O/CH<sub>4</sub> ratios = 1 and 2). There are little differences between the Ni(111) crystallite size in the catalysts at all H<sub>2</sub>O/CH<sub>4</sub> ratios.

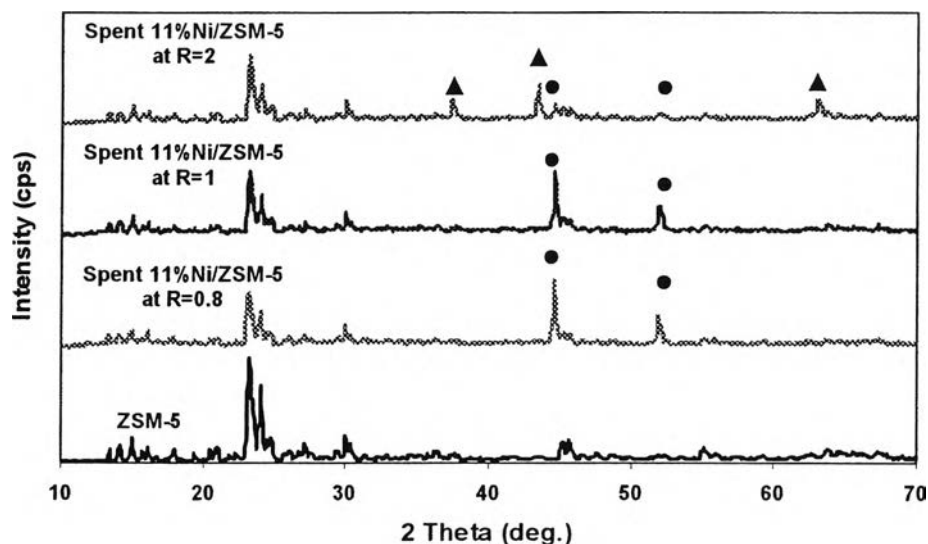


**Figure 4.15** XRD patterns of ZSM-5 zeolite and spent 11%Ni/ZSM-5 catalysts with various H<sub>2</sub>O/CH<sub>4</sub> ratios operated on steam reforming reaction at 700°C and atmospheric pressure for 5 hours; (▲), NiO phase; (●), Ni metal phase.

**Table 4.5** Metal crystallite sizes of spent 11%Ni/ZSM-5 catalysts with various H<sub>2</sub>O/CH<sub>4</sub> ratios

H <sub>2</sub> O/CH <sub>4</sub> ratio	NiO(111) (2θ = 37.3°) (nm)	NiO(200) (2θ = 43.3°) (nm)	NiO(220) (2θ = 63°) (nm)	Ni(111) (2θ = 44.5°) (nm)	Ni(200) (2θ = 51.8°) (nm)
R = 0.8	-	-	-	38.49	33.96
R = 1	-	-	-	36.06	28.03
R = 2	29.11	30.52	29.77	39.19	31.2

#### 4.2.2.3 Temperature Programmed Oxidation (TPO) and Thermal Gravimetric Analysis (TGA)

Since the carbon formation is considered to be a serious problem for this work, the temperature programmed oxidation (TPO) and Thermal Gravimetric Analysis (TGA) experiments were applied to determine the amount, location, and morphology of carbon deposited on the spent 11%Ni catalysts with various H<sub>2</sub>O/CH<sub>4</sub> ratios.

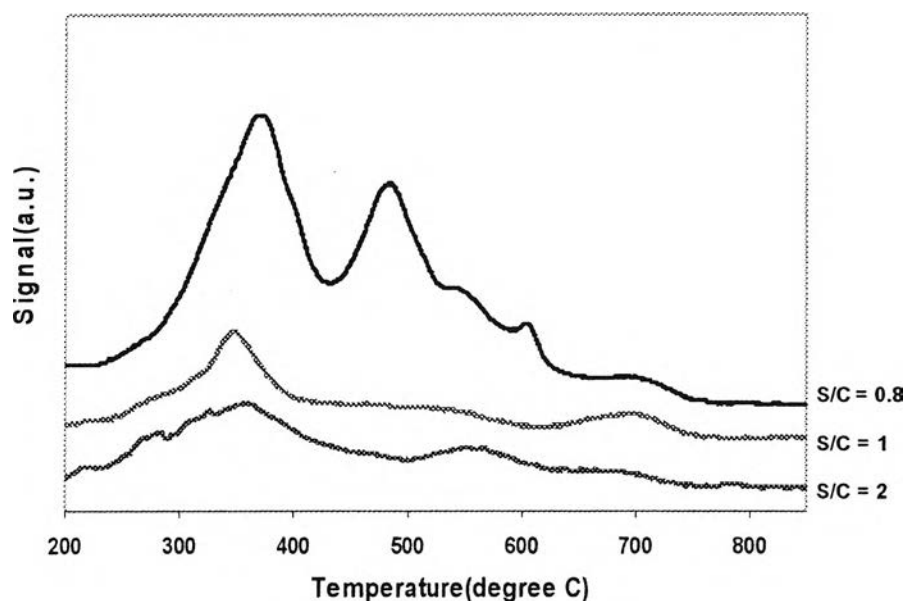


**Figure 4.16** TPO profiles of the Ni/ZSM-5 catalysts after 5 hours of reaction at 700°C and atmospheric pressure with various ratios of H<sub>2</sub>O/CH<sub>4</sub>.



**Table 4.6** Amounts of carbon deposited on 11%Ni/ZSM-5 catalysts with various H<sub>2</sub>O/CH<sub>4</sub> ratios after 5 hours of reaction, which were characterized by using TPO and TGA techniques

Catalyst	% wt Carbon <sup>(1)</sup>	% wt Carbon <sup>(2)</sup>
H <sub>2</sub> O/CH <sub>4</sub> = 0.8	0.57	0.53
H <sub>2</sub> O/CH <sub>4</sub> = 1	0.2	0.31
H <sub>2</sub> O/CH <sub>4</sub> = 2	0.22	0.26

<sup>(1)</sup> As measured by TPO

<sup>(2)</sup> As measured by TGA

Figure 4.16 shows the profiles obtained by TPO technique for several 11%Ni/ZSM-5 catalysts with different H<sub>2</sub>O/CH<sub>4</sub> ratios used in reforming process. According to the spent 11%Ni/ZSM-5 catalysts with the H<sub>2</sub>O/CH<sub>4</sub> ratios of 1 and 2 profiles, three peaks of different carbon species are observed. The first peaks with highest intensity are discovered at about 350°C which related to the high formation of carbide carbon species. Around 520-550°C, the second peaks which corresponding to the filamentous carbon are observed and these show the shift of the peaks compared to a TPO pattern of the catalyst with a H<sub>2</sub>O/CH<sub>4</sub> of 0.8 that has the second peak at 490°C. The other peaks are displayed around 700°C with low intensity. And, they are attributed to the pyrolytic carbon species as described previously. All TPO patterns show that an increased H<sub>2</sub>O/CH<sub>4</sub> ratio negatively impacted the intensity of peaks which involves the change of coke formation. In the case with excessive steam in the feed, the CO<sub>2</sub> signal is lower than that in case with a low level or proportional steam in feed.

Also, the catalyst has the higher total of deposited carbon at a H<sub>2</sub>O/CH<sub>4</sub> ratio = 0.8, whereas essentially lower amounts of deposited carbon were observed at H<sub>2</sub>O/CH<sub>4</sub> ratios of 1 and 2 that, as seen in Table 4.6. This is corresponding to Goud *et al.* (2007) work, which implied that S/C ratio is a critical parameter in enhancing the rate of reaction and minimizing the rate of deactivation.

The higher concentration of steam in the feed should translate into higher catalyst surface coverage by steam, as a result of the lower rate of deactivation which might also be due to higher extent of WGS reaction in the presence of excess steam. The present results prove this previous work, since the increasing steam concentration detracts the carbon content on the catalyst surface.

Furthermore, the TGA results as shown in the Table 4.6 can help to confirm the amounts of deposited carbon that were occurred on the catalysts and to understand the effect of the steam which has a function in the suppression of the carbon formation on these catalysts.

### 4.3 Effect of Ceria Content

The series of 11%Ni/ZSM-5 catalysts with various Ce loadings were studied in steam reforming of CH<sub>4</sub> at a H<sub>2</sub>O/CH<sub>4</sub> ratio of 0.8 in order to improve the performance of the Ni-based catalysts.

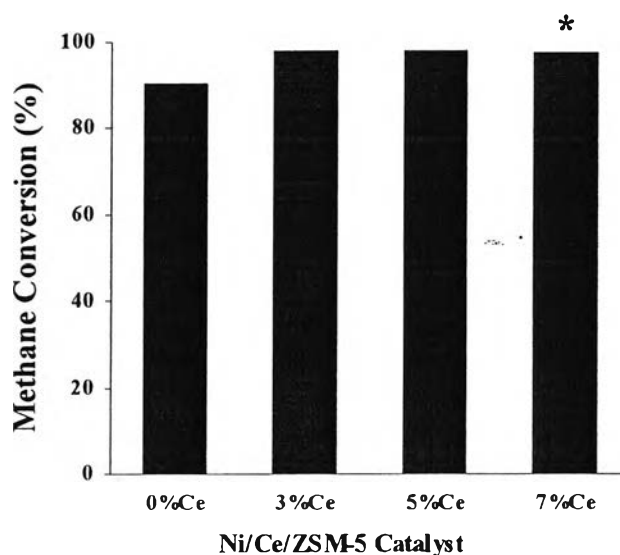
#### 4.3.1 Activity Test

The 11%Ni/ZSM-5 zeolite catalysts promoted with various CeO<sub>2</sub> contents (3, 5, and 7 wt%) were tested for the catalytic activity on reforming reaction at a H<sub>2</sub>O/CH<sub>4</sub> ratio of 0.8 and 700°C. Figure 4.17 presents the conversions of CH<sub>4</sub> at 5 hours time-on-stream over these catalysts. The CH<sub>4</sub> conversions of the 3% and 5% CeO<sub>2</sub> promoted catalysts show almost constant for 5 hours of reaction. And, their values are so close when the reaction reached the end. It is seen that there is a little difference on the catalytic performance of the 3% and 5%CeO<sub>2</sub> promoted Ni/ZSM-5 catalyst as compared to the unpromoted Ni/ZSM-5 zeolite catalyst. The stability of the Ni/ZSM-5 was found to be improved by the addition of CeO<sub>2</sub> into the catalysts. CH<sub>4</sub> conversions are increased by the CeO<sub>2</sub> addition (3 and 5 wt%), excepting for the 11%Ni/7%Ce/ZSM-5 catalyst which shows the dropping of CH<sub>4</sub> conversion since the first period of the reaction as 120 minutes. This is the consequence of the high carbon formation on this catalyst which lead to the plugging of the reactor after 120

minutes time-on-stream. Also, the high amounts of deposited carbon can be confirmed by the TPO and TGA characterizations as following.

These are parallel with the reported results in Crisafulli *et al.* (2002)'s paper that explained in the case of the addition of Ru as a promoter on supported Ni catalysts. It affects the catalytic performance towards the CO<sub>2</sub> reforming of methane.

Consequently, using the promoter is known as a way to improve the catalytic performance of the catalysts on reforming reaction and there are many species of the promoter which can be used in each suitable case.

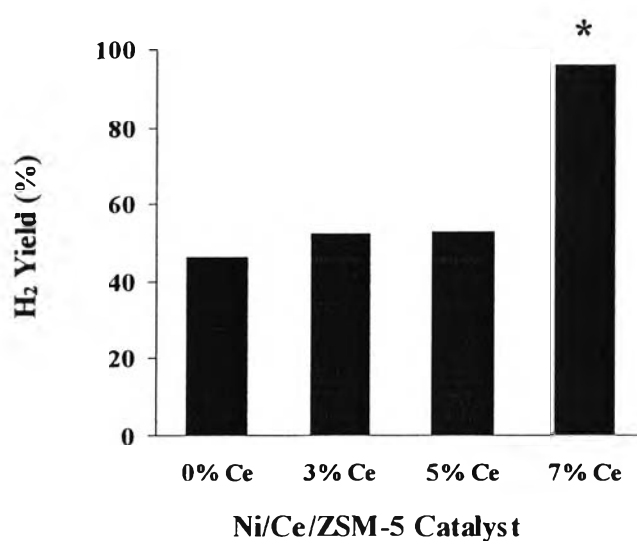


(\*) As measured at 120 minutes of reaction.

**Figure 4.17** CH<sub>4</sub> conversion at 5 hours time-on-stream over 11%Ni/ZSM-5 catalysts with different CeO<sub>2</sub> contents for steam reforming reaction at 700°C and a H<sub>2</sub>O/CH<sub>4</sub> ratio of 0.8.

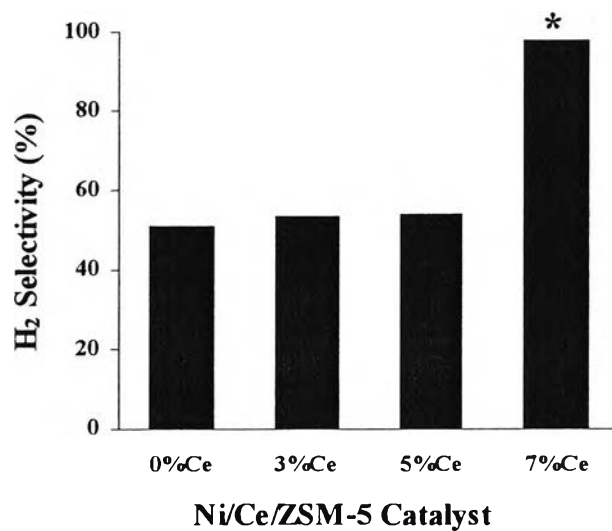
From Figure 4.18, the promoted catalysts exhibit the influence on the yield of H<sub>2</sub>. The H<sub>2</sub> yields of the 3 wt% and 5 wt% CeO<sub>2</sub> promoted catalysts remain constant throughout 5 hours of the testing time and also show the close values at the end of reaction (excepting with the 11%Ni/7%Ce/ZSM-5 catalyst). It shows that the addition of CeO<sub>2</sub> promotes the production of H<sub>2</sub> and the trends of H<sub>2</sub> yield and CH<sub>4</sub> conversion are the same.

In Figures 4.19 and 4.20, H<sub>2</sub> selectivity and CO selectivity at the end of reaction time are displayed, respectively. No existing of the effect of the promoted catalysts on H<sub>2</sub> selectivity (excepting for the 11%Ni/7%Ce/ZSM-5 catalyst), but there is a small difference in the selectivity of CO over the promoted and unpromoted catalysts (5.15% at the last of 11%Ni/ZSM-5).



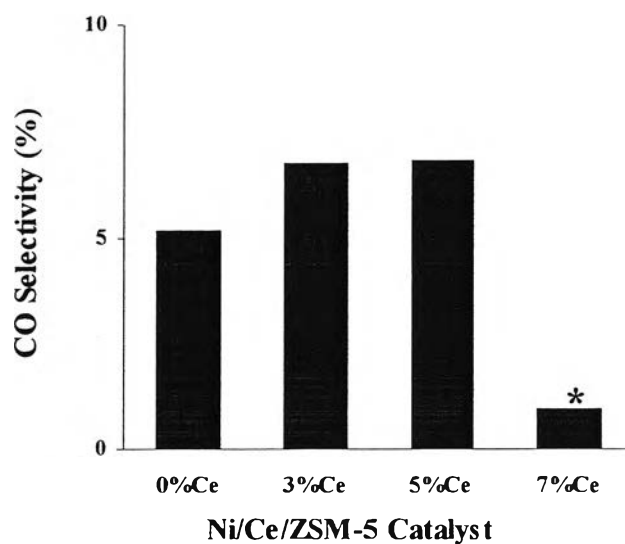
\*) As measured at 120 minutes of reaction.

**Figure 4.18** H<sub>2</sub> yield at 5 hours time-on-stream over 11%Ni/ZSM-5 catalysts with different CeO<sub>2</sub> contents for steam reforming reaction at 700°C and a H<sub>2</sub>O/CH<sub>4</sub> ratio of 0.8.



(\*) As measured at 120 minutes of reaction.

**Figure 4.19** H<sub>2</sub> selectivity at 5 hours time-on-stream over 11%Ni/ZSM-5 catalysts with different CeO<sub>2</sub> contents for steam reforming reaction at 700°C and a H<sub>2</sub>O/CH<sub>4</sub> ratio of 0.8.



(\*) As measured at 120 minutes of reaction.

**Figure 4.20** CO selectivity at 5 hours time-on-stream over 11%Ni/ZSM-5 catalysts with different CeO<sub>2</sub> contents for steam reforming reaction at 700°C and a H<sub>2</sub>O/CH<sub>4</sub> ratio of 0.8.

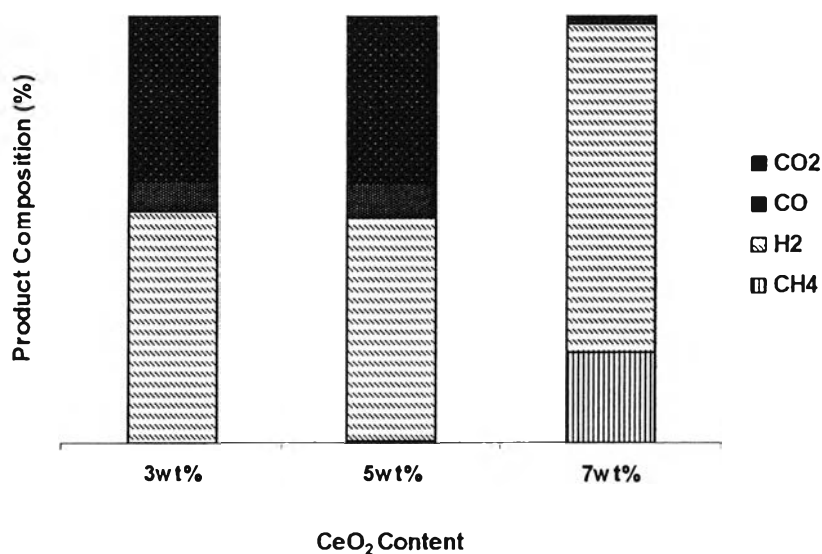


**Figure 4.21** Product Distribution of the 11%Ni/ZSM-5 catalysts with different CeO<sub>2</sub> contents operated on steam reforming reaction at 700°C and a H<sub>2</sub>O/CH<sub>4</sub> ratio of 0.8 for 2 hours.

Figure 4.21 shows the product gas distribution of the 11%Ni/ZSM-5 catalysts with different CeO<sub>2</sub> contents operated on the reforming reaction for 2 hours. While the product compositions of the 11%Ni/3%Ce/ZSM-5 and 11%Ni/5%Ce/ZSM-5 catalysts do not show significant difference at 2 hours of reaction, H<sub>2</sub> and CH<sub>4</sub> become the main compositions in the product gases of the 11%Ni/7%Ce/ZSM-5 catalyst at the same time. The appearance of the higher CO<sub>2</sub> composition in the 3wt% and 5wt% CeO<sub>2</sub> content catalysts reveals that the reduction of carbon formation can be promoted by the addition of CeO<sub>2</sub> which towards the combination of oxygen from CeO<sub>2</sub> and CH<sub>4</sub> in feed gas. On the other hand, the presence of CO<sub>2</sub> composition for the 11%Ni/7%Ce/ZSM-5 catalyst was rarely observed, this may confirm that too high CeO<sub>2</sub> content can not promote this reaction and can not help to inhibit the formation of coke.

The results from this part can be suggested that the presence of CeO<sub>2</sub> can help to produce more hydrogen on the steam reforming of methane at the suitable conditions. The promoted catalyst gives the higher activity and stability along the time of reaction due to more resistance to sintering and coking. While, the 3 wt% and 5 wt% CeO<sub>2</sub> addition to Ni/ZSM-5 catalysts enhanced the stability and

activity of Ni/ZSM-5 catalysts, the Ni/Ce/ZSM-5 catalyst added over or about 7 wt% of CeO<sub>2</sub> was deactivated more rapidly than the Ni/ZSM-5 catalyst without CeO<sub>2</sub> component, as explained by the characterizations in the previous part. These are corresponding with Laosiripojana *et al.* (2005) who noted that the doping of too high CeO<sub>2</sub> content results in the oxidation of Ni, which could reduce the reforming reactivity.

Finally, the results in all parts lead to several interesting conclusions which indicate that the 11%Ni/5%Ce/ZSM-5 catalyst shows the best catalytic performance in terms of activity and stability (along 12 hours time-on-stream). Furthermore, it is also revealed that the addition of CeO<sub>2</sub> promoter reduced the size of Ni species and produced the highly dispersed Ni species, and consequently, retarded the catalyst deactivation.

#### 4.3.2 Catalyst Characterization

The 11%Ni/ZSM-5 catalysts with different CeO<sub>2</sub> loadings which tested at a H<sub>2</sub>O/CH<sub>4</sub> ratio of 0.8 were characterized by ICP, XRD, TGA, TPO, and TEM methods to uphold the activity test results as followed.

##### 4.3.2.1 Inductively Coupled Plasma/Optical Emission Spectrometry (ICP/OES)

The elemental analyses (Ce and Ni) were performed by ICP as shown in Table 4.1. For the CeO<sub>2</sub> promoted catalysts, the actual loading and calculated values of the CeO<sub>2</sub> and Ni loadings also do not show a significant difference. This also agrees with Damyanova *et al.* (2002) work that studied for the characterization of ceria coated alumina carrier. It reported the actual % CeO<sub>2</sub> loadings via the ICP results and further showed no difference between the actual and calculated values.

##### 4.3.2.2 X-Ray Diffraction (XRD)

The XRD patterns of spent catalysts with various amounts of ceria promoter (CeO<sub>2</sub> loadings of 3, 5, and 7%) are expressed in Figure 4.22. A characteristic band at  $2\theta = 25^\circ$  ( $d = 3.56 \text{ \AA}$ ) was the main difference between the

spectra of the 11%Ni/7%Ce/ZSM-5 catalyst and the other promoted catalysts. This line corresponds to line (002) of pregraphitic carbon ( $d_{(002)} = 3.35 \text{ \AA}$ ) (Querini, 2004). These results indicate that the coke on the 11%Ni/7%Ce/ZSM-5 catalyst has indeed a certain degree of organization and 7 wt% is an overload of  $\text{CeO}_2$  loading for this catalyst due to the presence of an obvious carbon peak. Generally, coke structure can be characterized by XRD analysis that makes it possible to determine if there is coke with crystalline structure on the catalyst. However, this technique has low sensitivity in this system, since the carbon signal remains very weak even at very high coke ratio of the 11%Ni/7%Ce/ZSM-5 catalyst, which can be assured by the appeared TPO, TGA, and TEM results in Table 4.8 and Figure 4.24. Additionally, the appearance of  $\text{CeO}_2$  species can be correlated with the broadening and decreasing in the intensity of XRD patterns specific to crystalline Ni observed in this Figure 4.22. These observations (broadening/low intensity peaks) from the XRD patterns of crystalline species can be related to a less crystalline phase and well-dispersed Ni.

Table 4.7 states the Ni crystallite sizes of spent  $\text{CeO}_2$  promoted-11%Ni/ZSM-5 catalysts which carried on reforming reaction at a  $\text{H}_2\text{O}/\text{CH}_4$  ratio of 0.8 for 5 hours. These XRD measurements demonstrate that the Ni crystallite size, as measured by the diffraction line width, decreased with the higher loading of a promoter. It indicates that the presence of  $\text{CeO}_2$  on these  $\text{CeO}_2$ -containing catalysts favors the formation of dispersed Ni-metal particles as compared to the unpromoted catalysts which contain larger Ni-metal particles, and consequently, retards the sintering of Ni species on the catalyst surface in the Ni-Ce/ZSM-5 catalyst.



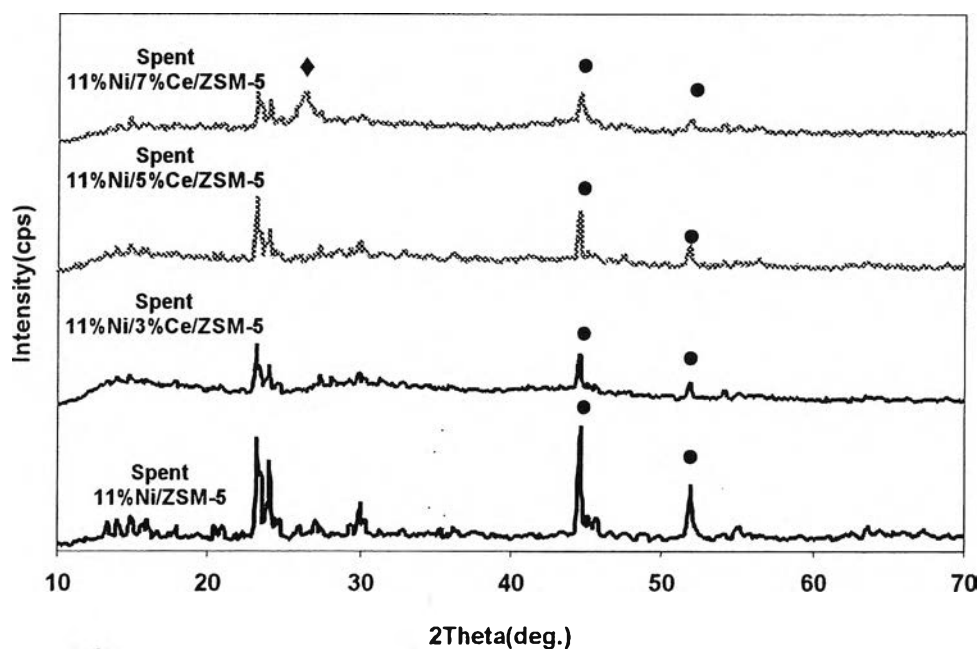


**Figure 4.22** XRD patterns of spent 11%Ni/ZSM-5 catalyst and CeO<sub>2</sub> promoted-11%Ni/ZSM-5 catalysts which operated on steam reforming reaction at 700°C and atmospheric pressure for 5 hours; (◆), C phase; (●), Ni metal phase.

**Table 4.7** Ni crystallite sizes of spent CeO<sub>2</sub> promoted-11%Ni/ZSM-5 catalysts with various amounts of CeO<sub>2</sub> loadings

Catalyst	Ni(111) ( $2\theta = 44.5^\circ$ ) (nm)	Ni(200) ( $2\theta = 51.8^\circ$ ) (nm)
unpromoted	38.49	33.96
11%Ni/3%Ce/ZSM-5	35.32	30.14
11%Ni/5%Ce/ZSM-5	37.48	25.30
11%Ni/7%Ce/ZSM-5	23.45	25.82

#### 4.3.2.3 Temperature Programmed Oxidation (TPO)

In order to analyze a CeO<sub>2</sub> promoter loading effect on the catalyst deactivation by coking, using TPO measurement is preferred. Figure 4.23

reproduces the profile results for two main peaks (around 350 and 500°C) of 11%Ni/ZSM-5 catalysts for which the CeO<sub>2</sub> had been added to 3%, 5%, and 7%wt (Because of a very high coke formation relative to the high CO<sub>2</sub> signal, which makes a profile of adding as 7 wt% ceria cannot involve in this figure). And, these peaks are identified as the superficial carbide and filamentous carbon species, respectively. Prior to the addition of CeO<sub>2</sub>, a significant decrease of the signal intensity of CO<sub>2</sub> is observed after increasing the contents of CeO<sub>2</sub> from 3 to 5wt%, which is relative to coking.

The considerable coke formation data on the steam reforming reaction over 11%Ni/ZSM-5 catalysts with several CeO<sub>2</sub> contents are exposed in Table 4.8. Previously, Craciun *et al.* (1998) implied that the deactivation of catalysts can occur through the loss of the oxygen-storage capacity, which is a significant property of CeO<sub>2</sub>. And, the deactivation has usually been explained as being due to a loss in the contact between CeO<sub>2</sub> and precious metal. The reported results are correlative to those, Table 4.8 shows interesting information in the difference of the deposited carbon quantities on 11%Ni/ZSM-5 catalyst without CeO<sub>2</sub> compared to CeO<sub>2</sub>-supported Ni catalysts. While the CeO<sub>2</sub> content was increased (for 3 and 5wt% CeO<sub>2</sub>), the formation of coke was inversely slow down. According to these TPO results, the agreement with Laosiripojana *et al.* (2005)'s research which studied the influence of the doping ceria on the resistance toward carbon formation on dry reforming of methane is shown. They found that the amount of carbon formation decreased with increasing Ce content as evidenced by TPO measurement.

Nevertheless, the limited loading of a CeO<sub>2</sub> promoter is noticed since the result showed the obviously large quantities of deposited carbon on 11%Ni/7%Ce/ZSM-5 catalyst, which may be explained by the disappearance of the O<sub>2</sub> transfer from CeO<sub>2</sub> to the precious metal. These results demonstrate that CeO<sub>2</sub> is a good promoter for this catalyst. It has the bifunctional mechanism to assist the reduction of coking, which is a main cause of the deactivation in this case, under the suitable range of loading.

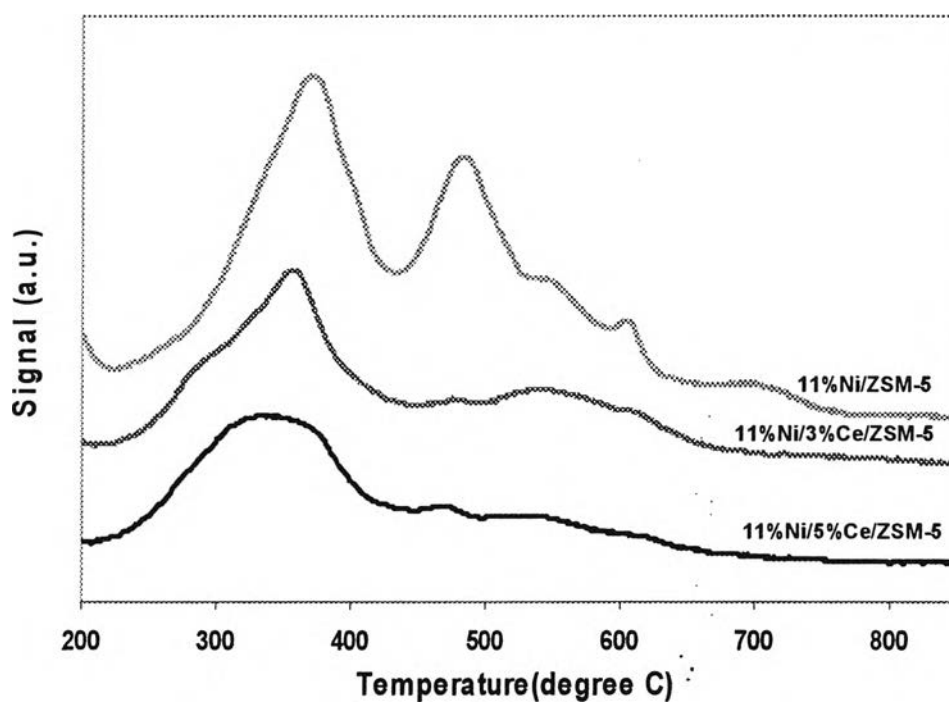


**Figure 4.23** TPO profiles of the Ni/ZSM-5 catalysts with several CeO<sub>2</sub> contents after 5 hours of reaction under 700°C, atmospheric pressure, and a H<sub>2</sub>O/CH<sub>4</sub> ratio of 0.8.

**Table 4.8** Comparison of the carbon deposited quantities between 11%Ni/ZSM-5 catalyst and CeO<sub>2</sub> promoted-11%Ni/ZSM-5 catalysts with several CeO<sub>2</sub> contents after 5 hours of reaction.

Catalyst	% wt Carbon <sup>(1)</sup>	% wt Carbon <sup>(2)</sup>
Unpromoted	0.57	0.53
11%Ni/3%Ce/ZSM-5	0.26	0.43
11%Ni/5%Ce/ZSM-5	0.22	0.79
11%Ni/7%Ce/ZSM-5	50.61	57

<sup>(1)</sup> As measured by TPO

<sup>(2)</sup> As measured by TGA

#### 4.3.2.4 Thermal Gravimetric Analysis (TGA)

As shown in Table 4.8, there is a little difference in the amounts of carbon deposited on 11%Ni/5%Ce/ZSM-5 which measured by TGA and TPO. While the TGA result revealed the increasing in carbon formation of the 11%Ni/5%Ce/ZSM-5 catalyst compared to the 11%Ni/ZSM-5 catalyst, which the amounts of carbon increased from 0.53 to 0.79 wt%, TPO measurement showed inverse data as 0.57 wt% decrease to 0.22 wt% carbon. This contrast may be explained by Querini's information which denoted that the result from the conventional TGA analysis is somewhat complicated due to weight changes caused by the oxidation of catalytic components and dehydration. And, this technique is also a sensitive technique to determine small amounts of coke.

#### 4.3.2.5 Transmission Electron Microscopy (TEM)

TEM images were taken for the spent CeO<sub>2</sub>-promoted catalysts (5% and 7% CeO<sub>2</sub> loading) after 5 hours reaction to examine the morphology of the catalysts, as shown in Figure 4.24. The TEM image of the 11%Ni/7%Ce/ZSM-5 shows the presence of tubular filament carbon with Ni particle at the end (Figure 4.24(b)). The mechanism of growth of carbon tubes is generally believed to involve diffusion of dissolved carbon in the Ni. Therefore, it was observed that carbon tube size was equivalent to or smaller than the Ni size (Lee *et al.*, 2004).

The numbers of carbon tubes with uniform sizes were observed on the spent 11%Ni/7%Ce/ZSM-5 catalyst, while carbon tubes just started to form on the spent 11%Ni/5%Ce/ZSM-5 catalyst. These TEM images are related to the results of deposited carbon quantities which measured by TPO and TGA techniques. It suggests that a very high carbon formation of the spent 11%Ni/7%Ce/ZSM-5 catalyst compared to the spent 11%Ni/5%Ce/ZSM-5 catalyst makes the deposited carbon easier to observe by TEM. The average particle sizes which calculated from previous equation for the spent 11%Ni/5%Ce/ZSM-5 and 11%Ni/7%Ce/ZSM-5 catalysts are 122.75 and 15.37 nm, respectively. And, the Ni particles of 66-145 nm were mainly observed by TEM on the spent 11%Ni/5%Ce/ZSM-5 catalyst surface. The present Ni particle size of the spent 11%Ni/7%Ce/ZSM-5 catalyst is parallel with the result from XRD measurement,

which indicates that the Ni crystallite size decreased with the addition of  $\text{CeO}_2$ . But, this TEM result of the spent 11%Ni/5%Ce/ZSM-5 shows the negative result compared to XRD result. However, the carbon growth rate can be related to the ability of metal particle segregation from the support by the observation of a large number of metal particles detached from the support. This supports that the presence of  $\text{CeO}_2$  promotes the dispersion of the metal on the surface of catalyst.

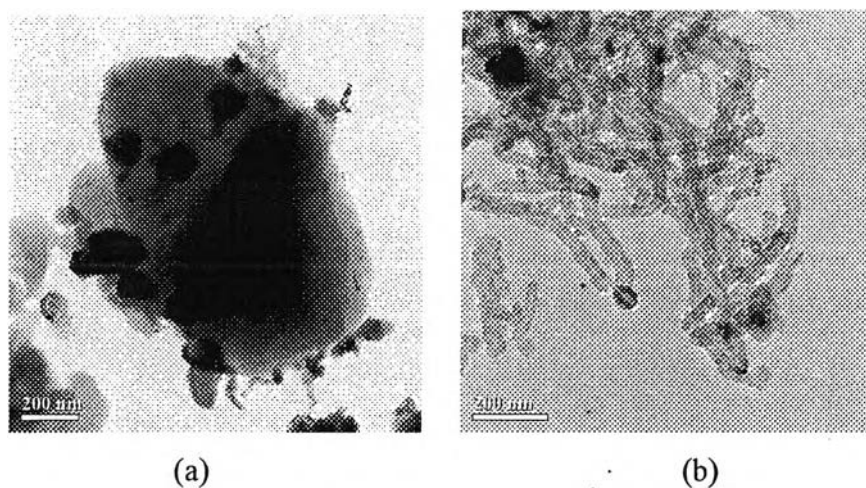


**Figure 4.24** TEM images of the catalysts after reforming reaction at 700°C; (a) 11%Ni/5%Ce/ZSM-5, (b) 11%Ni/7%Ce/ZSM-5.